Selection of Mechanical Properties for Virtual Mechanical Testing of Clinical Distal Femur Fractures

Maham Tanveer[1], Hannah Dailey[1]
[1]Lehigh University, Bethlehem, PA
mat422@lehigh.edu

Disclosures: Maham Tanveer (N), Hannah L. Dailey (4/5/6 – OrthoXel; ORS - 9)

INTRODUCTION: Clinical outcome measures for bone fracture healing rely heavily on radiographic scores, binary events such as nonunion or reoperations, and patient-reported measures such as physical function or quality of life. As a complement to these assessments, image-based virtual mechanical testing can provide extra insight into the biomechanics of fracture healing. This technique employs computed tomography (CT) scans to create patient-specific bone finite element models. In these models, the patient-specificity comes from the geometric representation of the bone and callus and the bone density, and in turn, the Young's modulus, derived from each voxel. Many equations for femoral bone density-to-modulus conversion have been proposed in the literature, leading to uncertainty about which approach is best in this context of use. Accordingly, the objective of this study was to test a wide variety of material laws found in literature to assess the capability of each for representing the mechanics of healing human distal femur fractures.

METHODS: Twenty distal femur fracture CT scans (ages 60-85; mixed male/female cohort, sex anonymized) from a previously published randomized control trial were used to create patient-specific finite element (FE) models [1]. The multi-center trial protocol was approved by the institutional review boards of all participating centers. CT scans were processed in Materialise Mimics and hexahedral meshes were created. To create a library of candidate material assignment laws, a literature review was performed identifying studies using elementwise material assignment laws in human femurs. Three equations were identified for converting CT scan Hounsfield units (HU) to calibrated mineral density (ρ_{QCT}), eight equations identified for converting ρ_{QCT} to ash density (ρ_{Ash}), six equations identified for converting ρ_{Ash} to apparent density (ρ_{App}), and eight equations converting one of the density measures to a Young's modulus (E) value. There was one equation that converted the raw CT HU units from the scan to a Young's modulus value. A total of 313 combinations of these equations were tested. Virtual torsional test was performed by fixing the distal end of the femoral diaphysis and applying a one-degree rotation at the proximal end along the longitudinal axis of the bone. Virtual torsional rigidity was calculated as $VTR = \frac{ML}{\phi}$, where M is the moment reaction at the distal end along the longitudinal axis of the bone, L is the length of the bone, and ϕ is the rotation. VTR was calculated for both fractured and reconstructed intact tibia to calculate a normalized value to assess healing $VTR_N = \frac{VTR_F}{VTR_I}$ (Fig. 1). To narrow down the list of viable equations to run on the FE models, a preliminary analysis was done to filter out equations with Young's modulus value above the experimentally known upper limit for intact cadaveric femurs: 25.5 GPa. To compare the results with different material models, three one-way ANOVAs (VTR_F, VTR_I, VTR_N) were performed with a p-value < 0.05 considered as statistically significant. The equation combinations were treated as categorical independent variable and the calculated VTR was considered as a continuous dependent variable.

RESULTS SECTION: Twenty-eight conversion equation combinations out of 313 candidate variations had maximum young's modulus value within the intact cadaveric femur range of 25.5 GPa. Comparison of predicted intact bone VTR_I with literature data for cadaveric intact femur torsional rigidity (3.35 ± 1.08 N-m^2/° [2], and 1.97 ± 0.89 N-m^2/° [3]) revealed that majority of the equation combinations had their interquartile range within the literature range. Statistical results showed a significant difference between the material model groups for both fractured VTR_F (Fig. 2; p < 0.001) and intact VTR_I (p < 0.001). However, no significant difference was found between the different combinations based on the normalized ratio VTR_N (Fig. 3; p = 0.289).

DISCUSSION: The results of this study demonstrated wide range of modulus (E) and torsional rigidity (VTR) values obtained from the different combinations of equations from literature. Among the material law combinations that produced physiologic-range results, normalization of the fractured torsional rigidity to intact (VTR_N) showed that any of the twenty-eight combinations of equations could be used to study healing outcomes, given that the output measure is VTR_N. From this list of candidate material models, one equation combination stood out as the best option for future studies on distal femur fracture. The equation combination 2-2--4 had the lowest percent difference (1.15%) between the mean intact torsional rigidity VTR_I and the intact cadaveric femur range from Papini et al. [3], which had age range similar to the patients from this clinical trial.

SIGNIFICANCE/CLINICAL RELEVANCE: This study showed that many realistic material properties models can be used from the literature to perform virtual mechanical testing as an outcome measure for healing, and that differences are minimized if the fractured models are normalized to the intact bone.

REFERENCES: [1] Lefaivre et al., J Bone Joint Surg Am., 106:1739-49 (2024), [2] Martens et al., JBiomech, 13, 667-676 (1980), [3] Papini et al., J Biomech Eng., 129, 12-19 (2007)

ACKNOWLEDGEMENTS: Thank you to Dr. Kelly Lefaivre and the University of British Columbia for access to the clinical data.

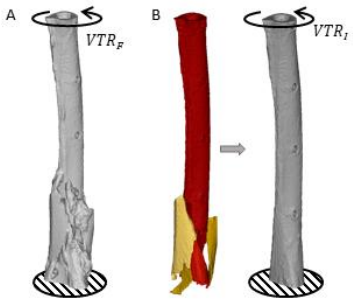

Fig. 1: (A). Fractured bones were segmented with their callus for VTR_F. (B) Fragments from the fractured bone were isolated and reconstructed into the intact bone for VTR_I.

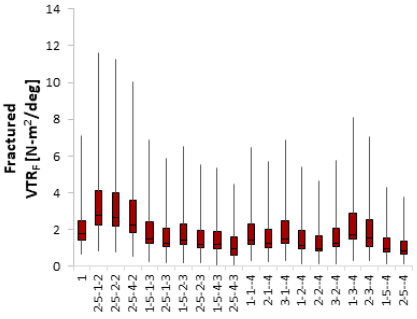

Fig. 2: Twenty representative combinations of equations showing fractured VTR_F for all twenty scans. Significant difference was found between the equation combinations in one-way ANOVA (p < 0.001).

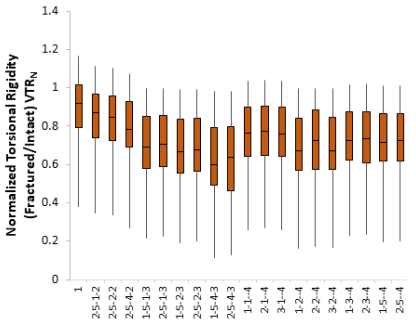

Fig. 3: Twenty representative combinations of equations showing normalized VTR_N for all twenty scans. No significant difference was found between the different combinations in VTR_N using one-way ANOVA (p = 0.289).